AFRL-AFOSR-JP-TR-2023-0030

Far-Field Electromagnetic Interference (EMI) Shielding Using Aperture-Controlled Skin-Core Beads Composite

Nam, Jae-Do
Sungkyunkwan University Research & Business
2066 Seobu-ro, Jangan-gu
Suwon,, , 16419
KR

11/06/2022
Final Technical Report

Air Force Research Laboratory
Air Force Office of Scientific Research
Asian Office of Aerospace Research and Development
Unit 45002, APO AP 96338-5002

REPORT DOCUMENTATION PAGE

PLEASE DO NOT RETURN YOUR FORM TO THE ABOVE ORGANIZATION.

1. REPORT DATE	2. REPORT TYPE	3. DATES COVERED	
20221106	Final	START DATE 20190429	END DATE 20210428

4. TITLE AND SUBTITLE
Far-Field Electromagnetic Interference (EMI) Shielding Using Aperture-Controlled Skin-Core Beads Composite

5a. CONTRACT NUMBER	5b. GRANT NUMBER	5c. PROGRAM ELEMENT NUMBER
FA2386-19-1-4056		61102F
5d. PROJECT NUMBER	**5e. TASK NUMBER**	**5f. WORK UNIT NUMBER**

6. AUTHOR(S)
Jae-Do Nam

7. PERFORMING ORGANIZATION NAME(S) AND ADDRESS(ES)
Sungkyunkwan University Research & Business
2066 Seobu-ro, Jangan-gu
Suwon, 16419
KR

8. PERFORMING ORGANIZATION REPORT NUMBER

9. SPONSORING/MONITORING AGENCY NAME(S) AND ADDRESS(ES)	10. SPONSOR/MONITOR'S ACRONYM(S)	11. SPONSOR/MONITOR'S REPORT NUMBER(S)
AOARD UNIT 45002 APO AP 96338-5002	AFRL/AFOSR IOA	AFRL-AFOSR-JP-TR-2023-0030

12. DISTRIBUTION/AVAILABILITY STATEMENT
A Distribution Unlimited: PB Public Release

13. SUPPLEMENTARY NOTES

14. ABSTRACT
Electromagnetic interference (EMI) shielding is the final defense for EMI problems that could impact almost all electrical and electronic systems from daily life to military activity and aerospace exploration. Although metallic barrier has been used for EMI shielding as a most popular way, it cannot ultimately eliminate EM waves but reflect and/or redirect them, which may very well impact the surrounding devices or bounce back to the detectors in the case of counter system development. Therefore, we believe that the EM-wave reflecting materials should be used along with the EM-wave absorbing materials to eliminate the reflected EM waves. For this purpose, we propose a mixture of two types of spherical skin-core beads, where the core bead is covered with either diffuse-reflection material (“conductor@bead”) or wave-absorbing material (“absorber@bead”). The spherical beads are quite advantageous in the task of EMI shielding because they redirect the waves repeatedly among the adjacent beads in the random direction until the EM wave sinks into the absorber. Furthermore, according to the theory of aperture shielding, the incident wave will be selectively prevented by the size-controlled aperture barrier, which can be ensured by the conformational arrangement of packed beads. The packed beads will be embedded in UV- or microwavecurable high-performance polymers, which would substantially increase the long-term durability of the EMI-shielding cover layer. Conclusively, we propose here a fundamental research on two different types of skin-core bead and the EMI shieling aperture of the beadincorporated composite providing a wide spectrum of material selection and fundamental knowledge in the various EMI shieling issues.

15. SUBJECT TERMS

16. SECURITY CLASSIFICATION OF:			17. LIMITATION OF ABSTRACT	18. NUMBER OF PAGES
a. REPORT U	b. ABSTRACT U	c. THIS PAGE U	SAR	22

19a. NAME OF RESPONSIBLE PERSON	19b. PHONE NUMBER *(Include area code)*
TONY KIM	315-227-7008

[Final Report]

Asian Office of Aerospace Research and Development (AOARD)

Far-Field Electromagnetic Interference (EMI) Shielding Using Aperture-Controlled Skin-Core Beads Composite

I. HEADING

A. Principal Investigator & Key Researcher

Name	Affiliation	Position
	Department	Field of Study/Final Degree
Jae-Do Nam (PI)	Sungkyunkwan University	Professor
	School of Chemical Engineering Department of Polymer Science and Engineering	Chemical Engineering/Ph.D.
Jonghwan Suhr (Co-PI)	Sungkyunkwan University	Associate Professor
	School of Mechanical Engineering	Mechanical Engineering/Ph.D.

B. Organization

Sungkyunkwan University

C. Award Number

FA9550-18-S-0003

PKG0024331 1

Tony Kim (IPO), Asian Office of Aerospace Research and Development (AOARD)

D. Award Title

Far-Field Electromagnetic Interference (EMI) Shielding Using Aperture-Controlled Skin-Core Beads Composite

E. Period of Performance:

05.01.2019 – 04.30.2021

II. SCIENTIFIC AND TECHNICAL OBJECTIVES

A. Major Goals

The goal of this project is to focus on the fundamental research of two types of skin-core beads ("conductor@beads" and "absorber@beads") and their high-performance composites for the development of a novel EMI shielding material system. The spherical beads could be quite unique in the task of EMI shielding because they redirect the waves repeatedly among the adjacent beads in the random direction until the EM wave sinks into the absorber (see the schematic in Fig. 1). We also investigated the fundamental principle of the aperture effect of the composite system that could be varied by such parameters as packing density, bead size, and ratio of conductor@beads and absorber@beads. A holistic approach is taken performing both analytical modeling and experimental measurement for the identification of property-processing-structure relationship of this novel composite system that is applicable in various EMI shieling issues.

This report presents the following works of the 2019-2021 reporting period of 1 May 2019 through 30 April 2021 as follows: (i) Frequency-selective EM wave absorption using two different types of skin-core beads of Ni@PMMA and Graphene@PS, (ii) Aperture control effects of ceria nanoparticles (bead size and coating thickness), (iii) Graphene@Ceria skin-core beads for EMI shielding, (iv) Preparation of MXene@PSGMA skin-core beads, and (v) Multilayer-structured Ag/h-BN/PEI composites for frequency-selective EMI shielding and heat dissipation.

In the first year, we achieved several significant scientific findings in frequency-selective characteristics, which are unique phenomena exerted by mono-sized spherical beads (i). In addition, ceria nanoparticles, a commonly-used corrosion-protective coatings, were selectively combined with graphene sheets, and provided a clear evidence of unified capability of corrosion protection and EMI shielding (ii, iii). During the second reporting period, we have established the preparation process of MXene nanosheet, which is considered as one of the best candidate materials for EMI shielding (iv). Furthermore, h-BN particles with skin-core structure have also been employed for polymer composite to provide multifunctional properties of EMI shielding, heat dissipation, and electrical insulation (v).

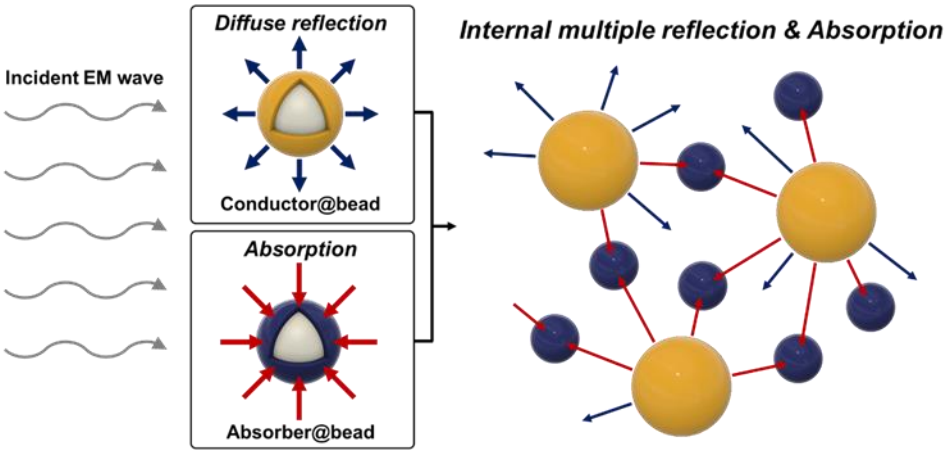

Figure 1. Schematic illustration of two different types of skin-core beads: diffuse reflection by "conductor@bead" and absorption by "absorber@bead." When these two beads are mixed in a composite structure, the redirected EM waves are absorbed and ultimately eliminated by the EM sink of absorber@beads.

B. Experimental

Various types of particles such as Ni@PMMA, Graphene@PS, ceria nanoparticles, Graphene@Ceria, and Ag@h-BN were synthesized and subsequently dispersed in polymer matrices with various weight ratios and fractions. The mixed pastes, which can be spary-coatable, were pressed at elevated temperatures for the measurement of EMI shielding and other analyses.

EMI shielding effectiveness (SE) of the prepared composites was measured in the X-band frequency range. The total EMI SE (SE_{Total}), absorption SE (SE_A), and reflection SE (SE_R) were calculated and the frequency-selective EMI shielding capability was identified.

To successfully conduct the research, we utilized cutting-edge devices available in our group's laboratory or as shared equipment facilities of the university. The experimental facilities for characterization include inductively coupled plasma mass spectroscopy, optical and electron spectrometers, Raman spectroscopy, scanning electron microscopy (SEM), high-resolution transmission electron microscopy (HR-TEM), vector network analyzer (VNA), X-ray diffractometer (XRD), differential scanning calorimetry (DSC), thermogravimetric analyzer (TGA), mechanical testing machine, and dynamic mechanical analyzer (DMA), and so on.

III. SUMMARIZED ACCOMPLISHMENTS

Approach I: Frequency-selective EM wave absorption using two different types of skin-core beads of Ni@PMMA and Graphene@PS

A. The single-layer intrinsic characteristics of skin-core bead composites containing Ni@PMMA and Graphene@PS beads were clearly analyzed. Subsequently, a bilayer structured composite composed of absorption layer and diffuse reflection layer exhibited an ultra-efficient EMI SE up to 69.0 dB with 96% of EM wave absorption, which stems from recursive internal diffuse reflection by Ni@PMMA beads.

B. EM wave absorption coating of a unique combination of bilayer composites attached on an aluminum plate eliminated up to 99.27% of the incident EM waves by absorption (reflection of only 0.73%).

C. The frequency-selective EM wave absorption in the bilayer composites was observed in the X-band frequency range. The absorption frequency and selectivity could be controlled by adjusting the ratio of the two types of skin-core beads.

Approach II: Aperture control effects of ceria nanoparticles (bead size and coating thickness)

A. Mono-sized spherical ceria nanoparticles could give precisely controlled aperture size for incident EM waves. The aperture was controlled by using nanoparticles of 100 and 300 nm, which could provide different frequency-selective EMI shielding capability.

B. As the loading content of ceria nanoparticles in composite increases, the EMI SE was increased and its peak frequency shifted to lower frequency region.

C. Regardless of the thicknesses between 1 and 5 mm, the frequency selectivity was clearly observed exhibiting an intact peak frequency at 9.62 GHz.

Approach III: Graphene@Ceria skin-core beads for EMI shielding

A. Ceria nanoparticles are often used for chemical corrosion protection with their switching capability of the oxidation states of Ce(Ⅲ) and Ce(Ⅳ), which makes it a good antioxidant. If graphene sheets are used along with ceria nanoparticles giving skin-core structured beads, the cooperation of induced dipole polarization of graphene and unique properties of ceria may serve synergistic effects for EMI shielding applications.

B. The EMI SE and EM wave absorption capability of Graphene@Ceria skin-core bead composites were measured with various weight fractions from 50% to 80%. The EMI SE of 8 dB and EM wave absorption of 65% were observed.

Approach IV: Preparation of MXene@PSGMA skin-core beads

A. MXenes ($Ti_3C_2T_x$) were successfully synthesized by using HF and MILD method. The negatively charged MXene nanosheets could cover the cationic polymer core (PSGMA) beads, yielding MXene@PSGMA skin-core beads, which can be used for EMI shielding materials.

B. Formation of the MXene@PSGMA beads were clearly confirmed by various analyses including SEM, TEM, and EDS elemental mappings.

Approach V: Multilayer-structured Ag/h-BN/PEI composites for frequency-selective EMI shielding and heat dissipation

A. Hexagonal boron nitride (h-BN) and silver coated h-BN (Ag@h-BN) particles were strategically chosen as fillers for multifunctional composites with their high thermal conductivity and electrically insulating/conducting properties.

B. Multilayer-structured composites were fabricated, which are composed of outermost electrically insulating layer and EMI shielding inner layer. They are containing different fillers of h-BN and Ag@h-BN particles for the target properties: electrical insulation and EMI shielding, respectively.

C. The Ag/h-BN/PEI composites exhibited high EMI SE up to over 60 dB with the unique frequency-selective EMI shielding capability, which could be controlled by adjusting the filler content. In addition, the composites also showed good thermal conductivity up to 7.61 W/mk.

IV. EXPANDED ACCOMPLISHMENTS

Approach I: Frequency-selective EM wave absorption using two different types of skin-core beads of Ni@PMMA and Graphene@PS

Fig. 2 depicts representative schematic of general procedure used in this work to prepare skin-core bead composites. The key issue is ultimate elimination of incident EM waves with synergistic effect of diffuse reflection from Ni@PMMA beads and absorption from Graphene@PS beads by regulating the ratio of the two different types of beads. The obtained skin-core bead composites were labeled Ni00/G00 (00 = from 10 to 70, corresponding to the weight fraction of the Ni@PMMA and Graphene@PS beads for the composites, respectively).

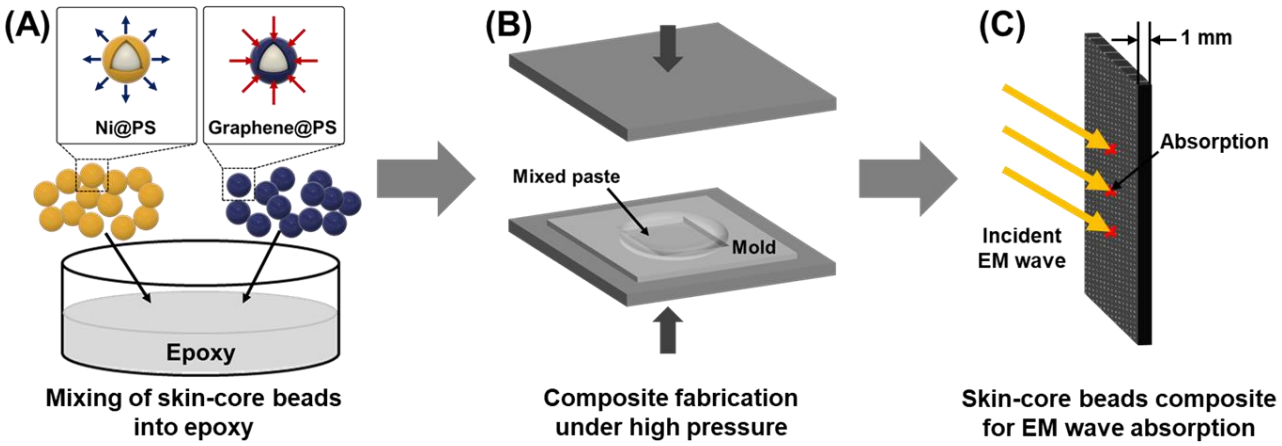

Figure 2. Schematic representation of the procedure used to fabricate the composites using two different types of skin-core beads of Ni@PMMA (Conductor@bead) and Graphene@PS (Absorber@bead): (A) Ni@PMMA and Graphene@PS beads were mixed into epoxy resin with different weight fractions and ratios; (B) the prepared paste was compression molded into sheets with curing the epoxy matrix; (C) the skin-core bead composites were obtained.

Our strategy for elimination of incident EM waves by absorption, not reflection is using bilayer-structured composites with a thickness of 2 mm composed of Ni00/G00 layer and G70 layer where the Ni00/G00 layer diffuse reflect and absorb the EM waves and G70 layer eliminate the residue EM waves completely by absorption. Fig. 3A shows the EMI SE of the bilayer composites in the X-band frequency range (8.2-12.4 GHz). With increasing weight fraction of the Ni@PMMA beads from 10% to 60% in the Ni00/G00 layer, corresponding to decreasing that of Graphene@PS beads from 60% to 10%, the average EMI SE increases from 4.7 to 64.7 dB where only 0.0000126% of EM wave is transmitted through the Ni60/G10+G70 bilayer composite. To clarify the EMI shielding mechanism in the composites, the total EMI SE (SE_{Total}), absorption SE (SE_A), and reflection SE (SE_R) at the frequency of 12.4 GHz are calculated and plotted in Fig. 3B. It is clear that the contribution of SE_R is negligible all over the bilayer composites exhibiting values under 3 dB. In particular, the SE_{Total}, SE_A, and SE_R value of the Ni60/G10+G70 bilayer composite are 69.0, 66.3, and 2.7 dB, respectively, which indicates that the contribution of absorption to the total EMI SE (96%) is much larger than that from reflection (4%), suggesting an absorption dominated

shielding mechanism. Our result is very interesting where absorption (SE_A) is increased with decreasing weight fraction of Graphene@PS and increasing weight fraction of Ni@PMMA considering that the carbon nanomaterials such as graphene absorb EM waves while metals reflect those. The ironic tendency may stem from internal multiple reflection by Ni@PMMA beads in the composites. As a result, our concept of the novel EMI shielding system is successfully verified where the synergistic effect of an absorber and a conductor eliminates incident EM waves by absorption.

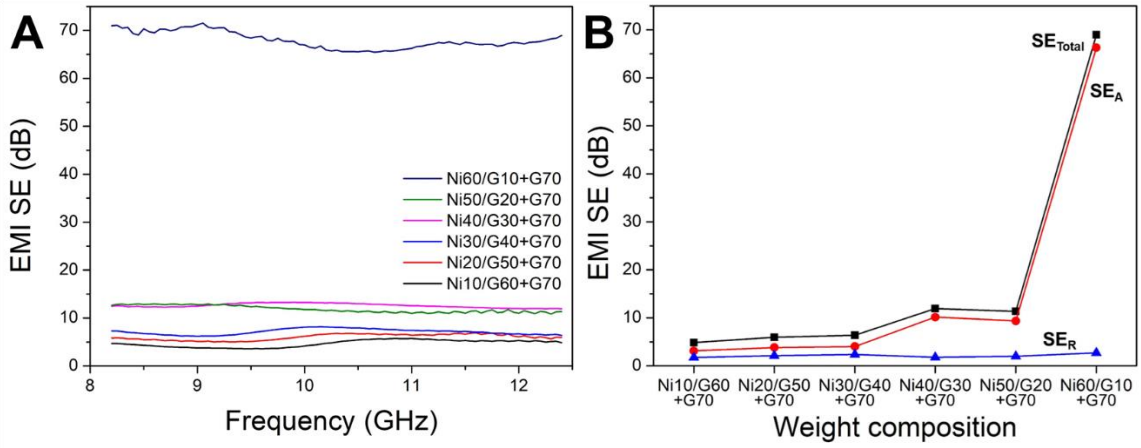

Figure 3. (A) EMI SE of bilayer composites with a thickness of 2 mm as a function of frequency in the X-band range. (B) Comparison of total EMI SE (SE_{Total}), absorption SE (SE_A), and reflection SE (SE_R) of the bilayer composites at the frequency of 12.4 GHz.

For the case of stealth system, we further developed the model of "EM wave absorption coating" with a thickness of 2 mm, as shown in Fig. 4A. The incident EM waves may be diffusely reflected by Ni@PMMA beads in the coating and ultimately eliminated by Graphene@PS beads. We set the measurement in the order of an absorption layer (G70), a diffuse reflection layer (Ni00/G00), and an aluminum foil as a metal substrate. In the EM wave absorption coating model, the transmission of the EM waves is negligible (≈ 0) due to entire reflection occurs on the surface of the metal substrate and thus the SE_{Total} and SE_A values calculated from transmittance term (T) are not applicable to this model in which EM waves are only reflected or absorbed. Accordingly, we used absorption fraction and SE_R values to identify the ratio of absorption and reflection. Fig.4B shows the absorption fraction of the bilayer coatings. The absorption fraction of the bilayer coatings is frequency-dependent exhibiting quite different values across the frequency range of X-band. For example, the highest absorption fraction of the Ni20/G50+G70 bilayer coating is 85.9% at the frequency of 10.45 GHz while the lowest value of that is 44.3% at the frequency of 8.2 GHz. In the case of Ni50/G20+G70 bilayer coating, the absorption fraction in the measured frequency range is higher than 75%. Especially, it eliminates almost all EM waves by absorbing 99.3% of the total amount at the frequency of 10.75 GHz, which means that only about 0.7% of EM wave is reflected. The SE_R curves of the coatings are shown in Fig. 4C. The shapes of the graphs are reversed compared with those of the absorption fraction where the lower the SE_R values, the more EM wave is

absorbed. The graph of Ni50/G20+G70 is the lowest than the other graphs exhibiting the lowest SE_R value of 0.031 dB at the frequency of 10.75 GHz.

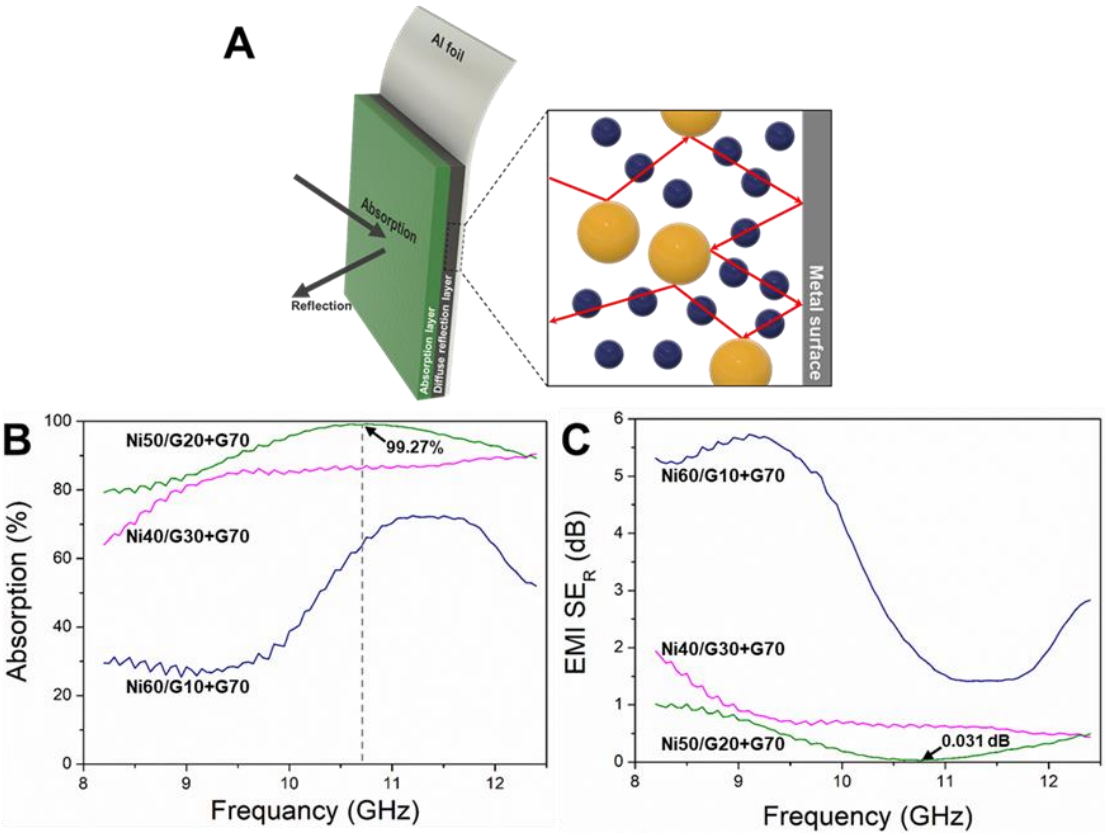

Figure 4. (A) The evaluation model of "EM wave absorption coating" and EM wave elimination mechanism on the surface of a metal substrate by the skin-core bead composite. (B) Absorption fraction and (C) SE_R of EM wave absorption coatings as a function of frequency in the X-band range.

The frequency-selective EMI shielding was also investigated by varying the ratio of the Ni@PMMA and Graphene@PS beads in the composites. We found that when the graphs of absorption fraction of the bilayer composites were plotted as a function of frequency, each graph has a peak of the highest absorption, which means that the composites can be used to selective EMI shielding by absorption as shown in Fig. 5A. We labeled the peaks f_{peak}. The f_{peak} of the Ni40/G30+G70 bilayer composite is 9.6 GHz with absorption fraction of 69.1% while that of the Ni60/G10+G70 is 11.3 GHz with absorption fraction of 76.1%. To specify selective absorption of the bilayer composites, we defined absorption selectivity and absorption selectivity parameter as:

$$\text{Absorption selectivity} = \frac{A}{A_{min}}$$

$$\text{Absorption selectivity parameter } \alpha = \frac{A_{max}}{A_{min}}$$

where A is absorption, and A_{min} and A_{max} are minimum and maximum value of absorption in the measured

frequency range, respectively. Fig. 5B shows the f_{peak} values and the absorption selectivity parameters (α) of the bilayer composites. Interestingly, the both values have a tendency dependent on the weight composition of the diffuse reflection layer (Ni00/G00). Accordingly, we can selectively use the composites in order to block incident EM waves at a desired frequency in the X-band. The α decreases as the weight fraction of Ni@PMMA beads increases from 10% to 50% with corresponding to decreasing weight fraction of Graphene@PS beads from 60% to 20%. In the case of Ni60/G10+G70 bilayer composite, it has the highest value of α of 2.82 where the composite absorbs the EM wave 2.82 times at 11.3 GHz of f_{peak} than least absorbed amount in the X-band range. The frequency selective EMI shielding capability stems from the specific ratio of Ni@PMMA and Graphene@PS beads for the composites and this may be only achieved when the spherical beads are used.

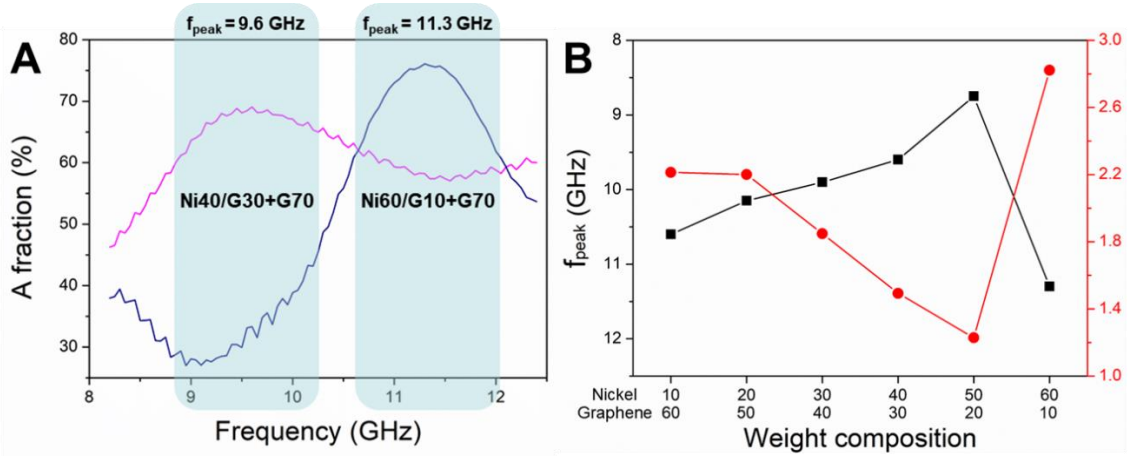

Figure 5. (A) Absorption fraction of the bilayer composites as a function of frequency in the X-band range. (B) f_{peak} and absorption selectivity parameter (α) as a function of weight composition of the diffuse reflection layer (Ni00/G00) in the bilayer composites.

Approach II: Aperture control effects of ceria nanoparticles (bead size and coating thickness)

EMI shielding is an ability of attenuating the EM waves by reflection or absorption with materials (Fig. 6A). EMI SE is different depending on the type of material, thickness, frequency, distance, etc. At the same frequency, the EMI SE could vary with the "aperture," which is specified by the distances between the fillers in the composite. Fig. 6B depicts correlation between aperture and incident EM waves; when the aperture between the fillers is larger than 1/2 wavelength, SE decreases because of the leakage of incident EM waves. Therefore, it is important to control the aperture size, which can be adjusted to the size, shape, and content of the fillers.

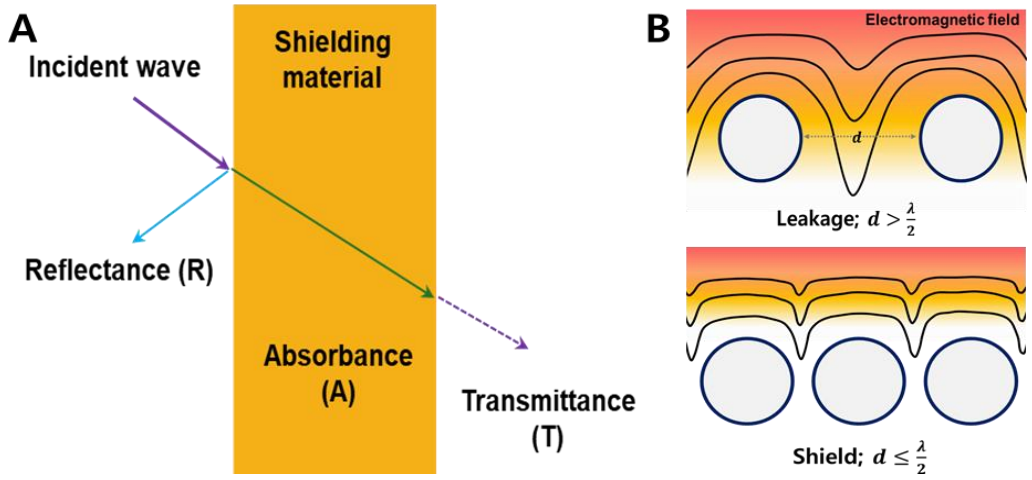

Figure 6. (A) Schematic representation of EMI Shielding. (B) Correlation between the aperture size in composites and incident EM waves in wide spectrum of frequency.

Ceria nanoparticles, which are widely used for surface coating materials to prevent corrosion, were synthesized as fillers for composites. The mono-sized ceria nanoparticles with sizes of 100 and 300 nm have spherical shape and highly narrow size distribution, as shown in Fig. 7A and 7B. They could give precisely controlled aperture size for incident EM waves.

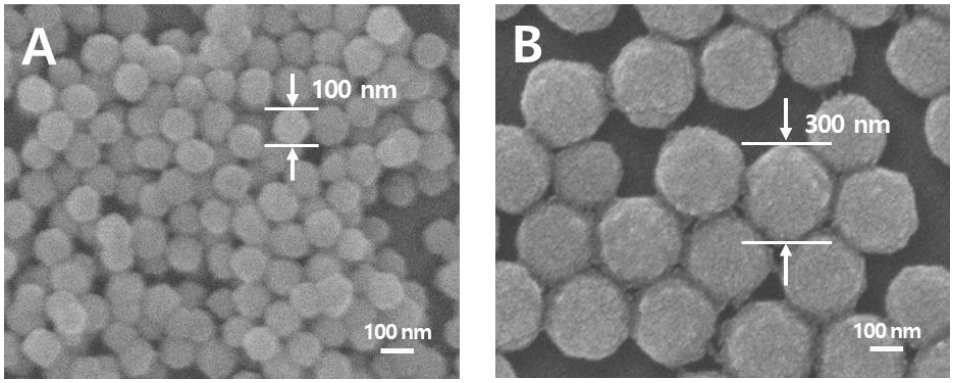

Figure 7. SEM images of spherical ceria nanoparticles used as fillers with sizes of (A) 100 nm and (B) 300 nm.

The EMI SEs with different particle size are provided in Fig. 8A, showing frequency-selective EMI shielding. Some peaks can be observed in different frequency ranges. For instance, the maximum EMI SE values of 100 nm-ceria composite are 3.51 and 4.21 dB at 9.21 and 10.24 GHz, respectively. On the other hand, 300 nm-ceria composite exhibits the maximum EMI SE values of 3.53 dB at 9.62 GHz. Fig. 8B shows the effect of different content of ceria nanoparticles (50, 60, and 70 wt%) in composites. As the loading content of ceria nanoparticles in composites increases, the EMI SE increases and the peak shifts to lower frequency region. Interestingly, the frequency selectivity of the composites is independent to sample thickness (Fig. 8C), while the EMI SE of the 300 nm-ceria composites at 9.62 GHz increases with the thickness (Fig. 8D).

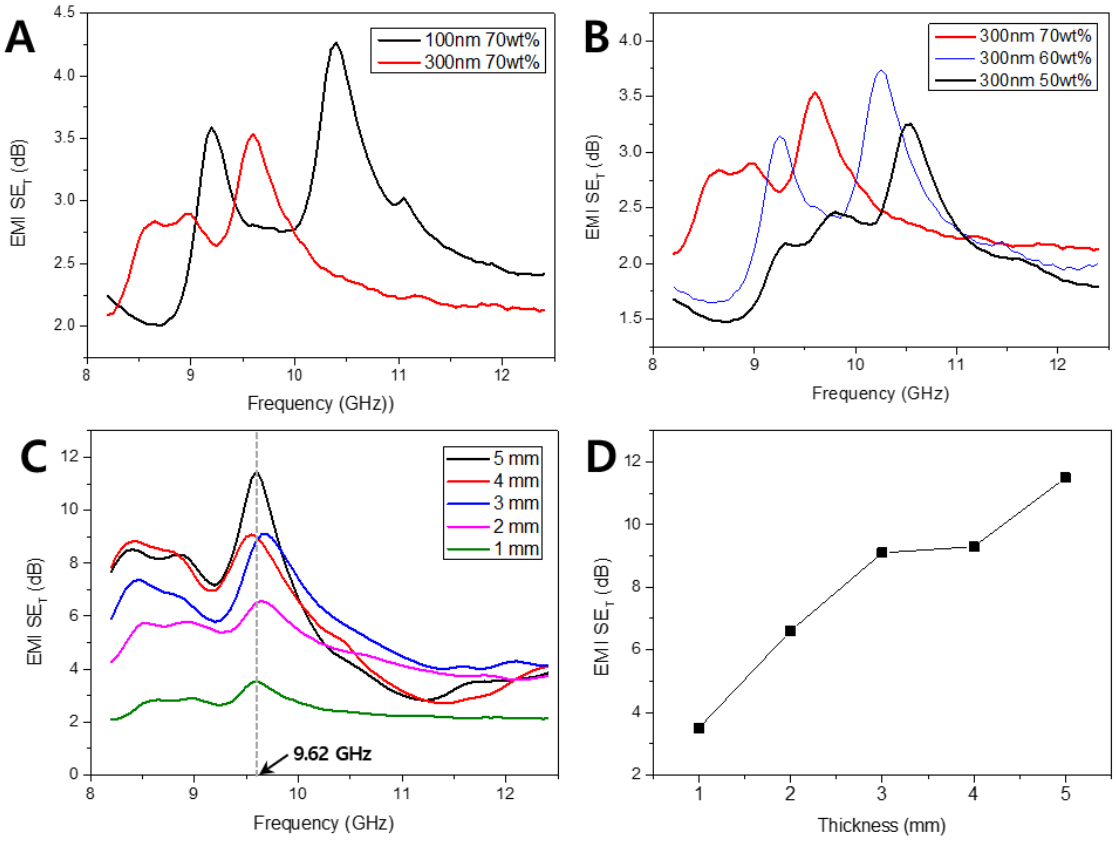

Figure 8. Comparison of EMI SE of ceria composites with (A) different particle size, (B) filler content (sample thickness: 1mm), and (C) sample thickness in the X-band frequency range. (D) EMI SE of 300 nm-ceria composites with various sample thickness at 9.62 GHz.

Approach III: Graphene@Ceria skin-core beads for EMI shielding

With high dielectric constant and stable electronic state of Ce(III) and Ce(IV), ceria has a strong oxidizing property. If graphene nanosheets are used along with the ceria nanoparticles with skin-core structure, ceria may induce dipole polarization of graphene owing to its oxidizing property, exhibiting enhanced EMI shielding property. Here, we propose EMI shielding characteristics of Graphene@Ceria skin-core beads. The fabrication process of the Graphene@Ceria beads is illustrated in Fig. 9. The negatively charged graphene oxide (GO) layer is self-assembled on the cationic surface of ceria nanoparticles via electrostatic attraction. Then, the GO layer was chemically reduced using hydrazine. Fig. 9B and 9C are SEM images of commercially available ceria nanoparticles (Solvay, Belgium) and Graphene@Ceria beads, respectively. The surface of Graphene@Ceria beads are very rough and wrinkled with a number of connected sites, verifying that the graphene nanosheets are covering the ceria particles.

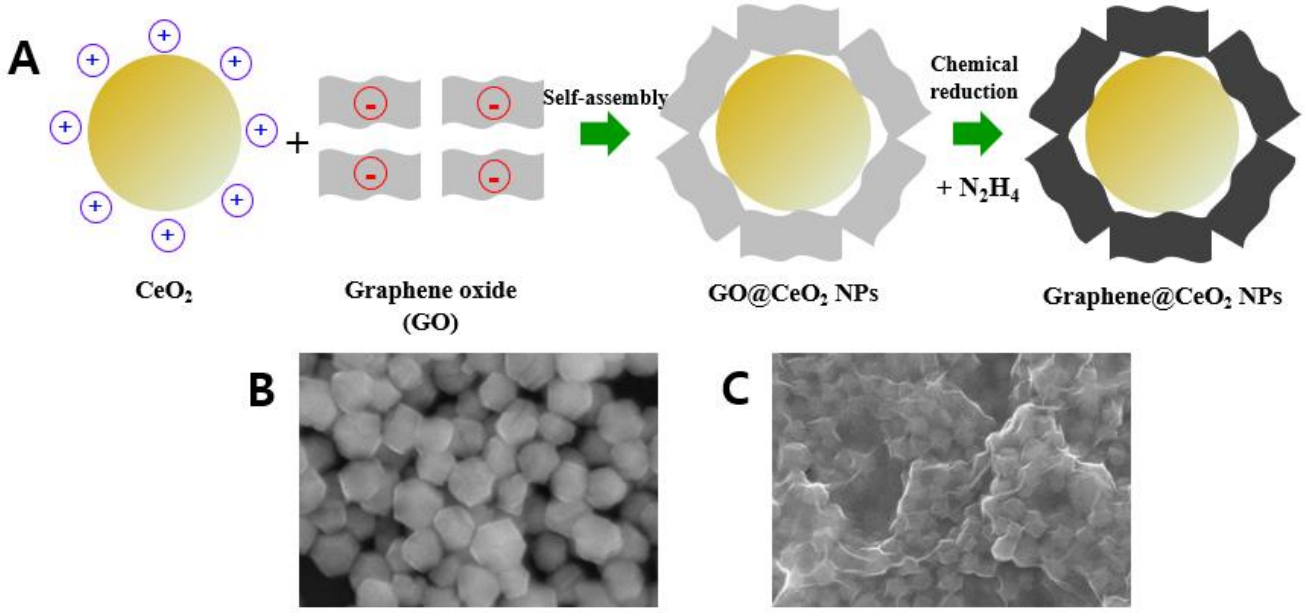

Figure 9. (A) Schematic representation of procedure used to prepare Graphene@Ceria beads. SEM images of (B) ceria nanoparticles and (C) Graphene@Ceria.

Fig. 10A shows zeta potential of the ceria nanoparticles, GO sheets, and Graphene@Ceria beads. With difference of surface charge, the GO layer could be self-assembled on the surface of ceria particles until the surface charge is neutralized. Fig. 10B shows Raman spectra of GO@Ceria and Graphene@ceria (reduced graphene oxide), providing two typical Raman peaks of G and D. The G peak at about 1600 cm^{-1} corresponds to one-phonon Raman scattering process at the first Brillouin zone center and consists of the collective in-plane bond stretching of the polyaromatic carbon atoms. The D peak at about 1400 cm^{-1} originates from the breathing modes of six-membered rings and its activation resonance process involves peculiar electron-phonon interaction mediated by defects. Therefore, after the chemical reduction, GO layer seems to be graphitized and thus conductive.

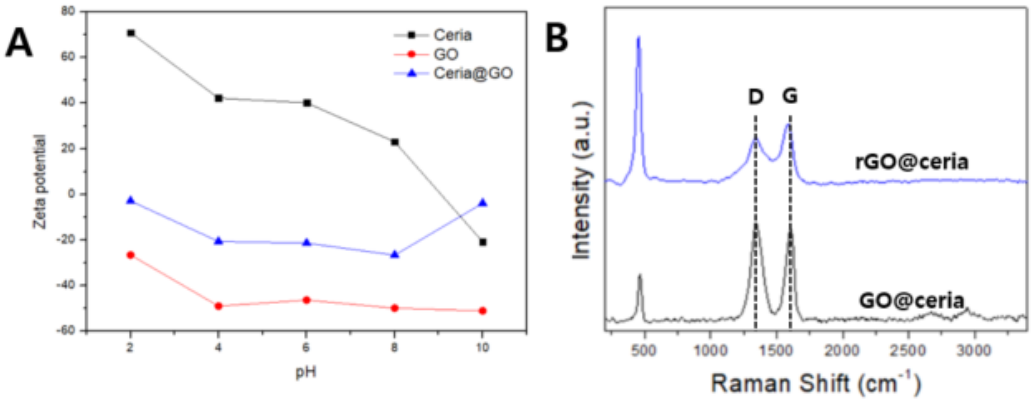

Figure 10. (A) Zeta potential of ceria nanoparticles, GO sheets, and GO@ceria beads. (B) Raman spectra of the GO@Ceria and Graphene@Ceria beads.

We plotted SE_{Total}, SE_A, and absorption fraction of the Graphene@Ceria skin-core beads composites as a function of frequency in the X-band with different filler content from 50% to 80% (Fig. 11). The average SE_{Total}, SE_A and absorption fraction increases with filler content from 3.85 dB to 7.8 dB, 2.2 dB to 4.5 dB, and 37% to 65%, respectively.

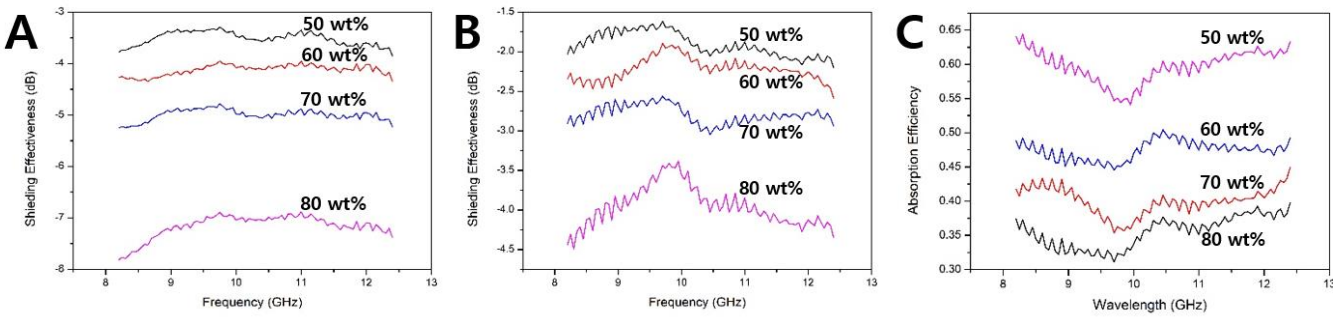

Figure 11. (A) SE_{Total}, (B) SE_A, and (C) absorption fraction of Graphene@Ceria skin-core bead composites with 1mm thickness in the X-band frequency range.

Approach IV: Preparation of MXene@PSGMA skin-core beads

In second year, we have established the fabrication process of MXene nanosheet, which is considered as one of the best EMI shielding materials with its 2D structure and high electrical conductivity (10,600 S/cm). MXene can be synthesized by a top-down etching process from MAX phase, which has layered structure composed of early transition metal (M), IIIA or IVA groups (A), and carbon or nitrogen (X). By etching the MAX phase using strong acid such as hydrofluoric acid (HF) and hydrochloric acid (HCl), the A group is eliminated and the remained weakly-bonded MX layers are additionally delaminated, providing 2D structure MX layers, which is called "MXene" to emphasize its graphene-like morphology. The MXene has hydrophilic property with negatively charged surface derived from its F, Cl, or OH terminal groups (T), and has high electrical conductivity arises from the high electron density of states near the Fermi level as predicted from density functional theory. We believe that the MXene nanosheets ($Ti_3C_2T_x$) can be employed as a skin material for skin-core beads for EMI shielding applications owing to their good processability and high electrical conductivity.

Typically, the MXene nanosheets can be synthesized mainly by two methods; the A layer is removed by using HF as an etchant or by Minimally Intensive Layer Delamination (MILD) method. Since the MXene nanosheets exhibit different properties depending on the synthesizing method, we investigated both methods giving various types of MXenes. For example, when HF was used for synthesis, we could obtain relatively small lateral-sized MXene nanosheets. Fig. 12 shows our MXene sheets, which were synthesized from the MAX phase compared with its ideal schematics of the lattice structure. The nanosheets are successfully exfoliated as shown in the SEM images. The additional SEM images of synthesized MXene particles are given in Fig. 13.

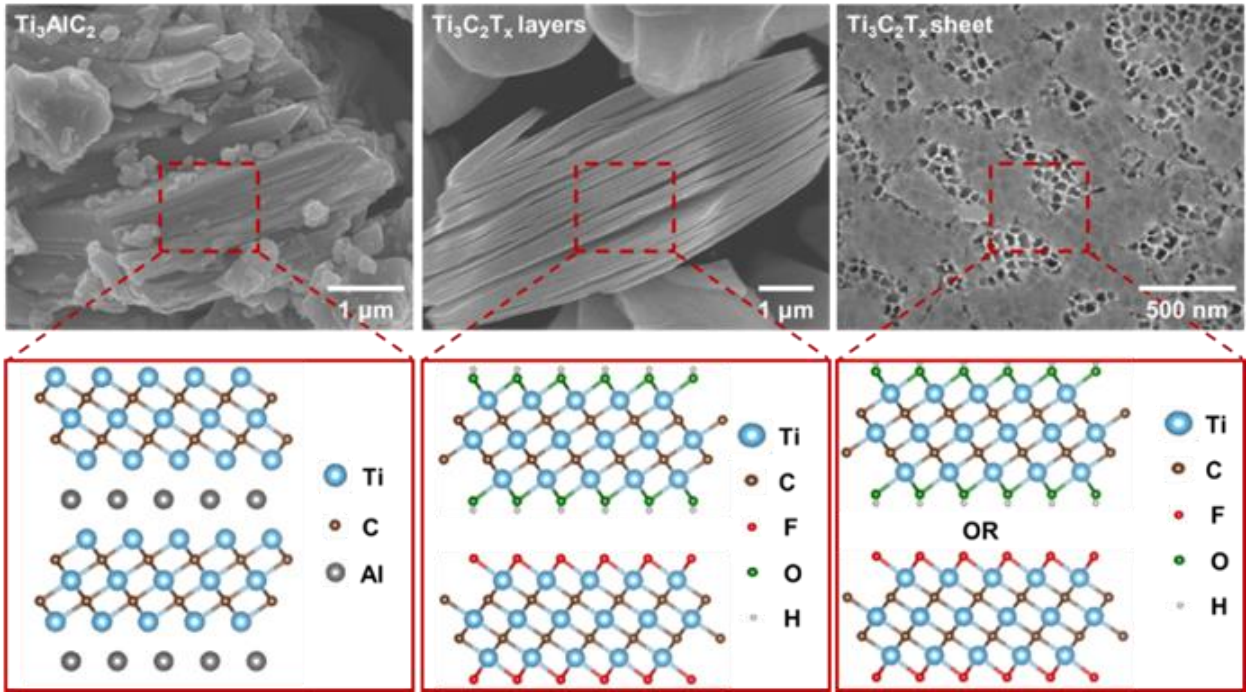

Figure 12. SEM images and schematic structures of MAX phase (Ti_3AlC_2), weakly bonded MXene ($Ti_3C_2T_x$) layers, and delaminated MXene ($Ti_3C_2T_x$) nanosheets.

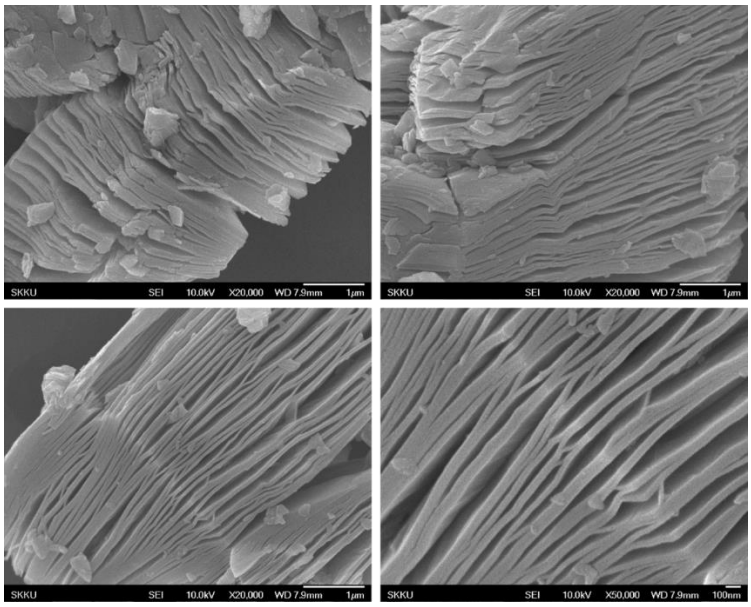

Figure 13. SEM images of various MXene particles at different magnifications.

As we prepared Graphene@PS beads via electrostatic self-assembly of positively charged graphene sheets on negatively charged PS cores in first year, MXene skin-core beads could be prepared by the same way. Since the MXene has negative charges in nature, we selected poly(styrene-co-gylcidyl methacrylate) (PSGMA) beads as a core material to fabricate the skin-core beads, which can be surface-modified to have positive charges. The MXene@PSGMA beads are mono-dispersed with an average diameter of 2 μm, exhibiting very rough surfaces. The presence of MXene shells on the polymer cores is clearly confirmed by SEM (Fig. 14). The surface of the MXene-wapped PSGMA beads is wrinkled and rough due to the thin MXene nanosheets.

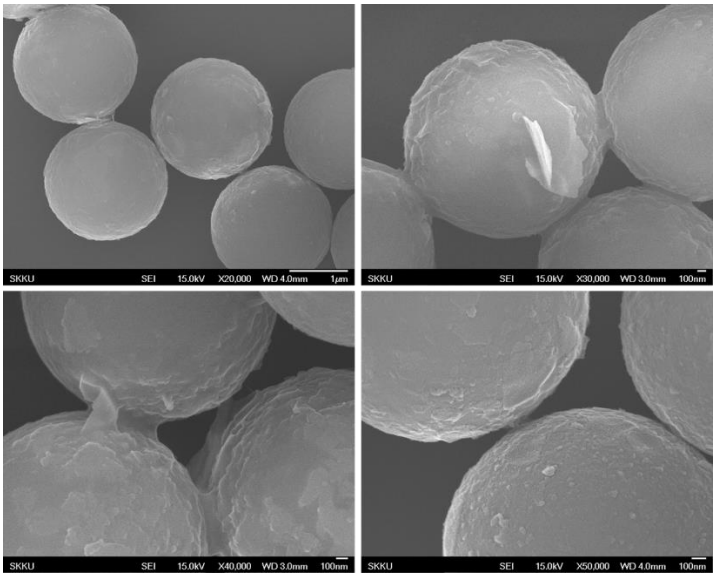

Figure 14. SEM images of our MXene@PSGMA beads at different magnifications.

In addition, TEM image and corresponding EDS elemental mappings of the MXene@PSGMA beads are shown in Fig. 15. The phase maps of C, N, Ti, and O in the figure show a good match with the TEM image, clearly demonstrating the formation of MXene@PSGMA beads. In particular, the presence of Ti can be seen, which is originated from the MXene ($Ti_3C_2T_x$) nanosheets. We will use the skin-core beads as a "conductor@bead" for the next project focusing on the frequency-selective EMI shielding applications.

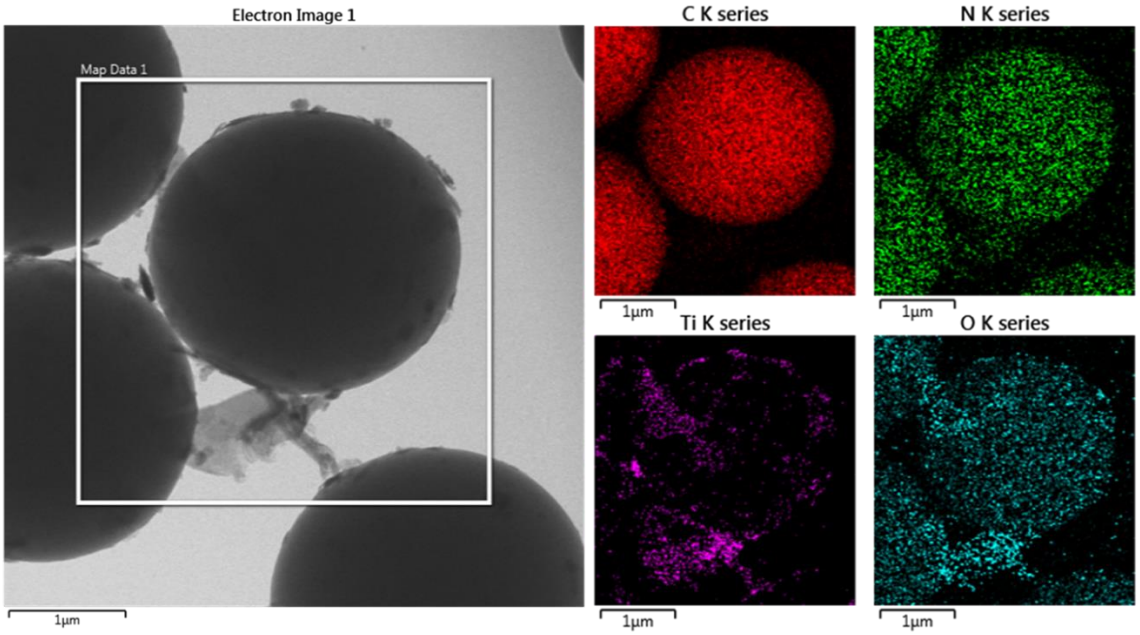

Figure 15. TEM image and corresponding C, N, Ti, and O EDS elemental mapping of MXene@PSGMA beads.

Approach V: Multilayer-structured Ag/h-BN/PEI composites for frequency-selective EMI shielding and heat dissipation

With the miniaturization and high integration of the electronic components for high speed and performance, both EMI shielding and thermal management have become crucial issues for modern electronic devices, setting higher and stricter requirements. Although the EMI problem can be resolved by typical EMI shielding materials, simultaneously dealing with heat dissipation in a single material is another issue, making much more complicated problems. With the dense packing of the electronic components, high heat fluxes are generated and accumulated, which adversely affect the proper operation of devices and the stability of the EMI shielding materials, subsequently reducing lifetime of the devices.

Furthermore, to use the materials for many electronic packaging applications such as molding compounds, high electrical insulation is required for isolating electronic components and interconnects. However, high EMI SE theoretically requires outstanding electrical conductivity (at least 1 S/m) of materials, and thus it seems that the electrical insulation cannot be achieved without inevitably sacrificing the EMI shielding performance of materials. Consequently, a novel multifunctional material system has now become essential, which can provide excellent EMI shielding, high thermal dissipation, and electrical insulation properties.

For the task of EMI shielding and heat dissipation, polymer composites with embedded electrically and thermally conductive fillers have been intensively explored in recent years, respectively, due to their lightweight, excellent processibility, low cost, and flexibility for material system design. For instance, metallic particles, MXene, graphene, and carbon nanotubes (CNTs) are usually selected as fillers for conductive composites, which attenuate incident EM waves by reflection and absorption with their charge carriers. In addition, they also exhibit high thermal conductivity. However, they are intrinsically electrically conductive and thus are inappropriate for filler in insulating composites. Meanwhile, although electrically insulating ceramic fillers are typically used for thermally conductive composites such as aluminum oxide, aluminum nitride, boron nitride, silicon nitride, etc., they cannot shield incident EM waves since they are not electrically conductive. Notably, much different types of fillers have been embedded in polymers for different functions, which makes it difficult to develop a multifunctional material with both EMI shielding and heat dissipation properties. Therefore, if electrically conductive materials are coated on heat dissipating materials, they will not only shield the incident EM waves, but also exhibit good thermal dissipation property with reduced interfacial thermal resistance.

In particular, the layered structure would be also employed for the polymer composite because it is one of the best structures that can give multifunctional properties, where the outermost layers are composed of insulating material while the inner electrically conductive layer can shield incident EM waves. In addition, we expected that the multilayer structured composite could exert the frequency-selective EMI shielding capability, as we identified that the unique functionality can be achieved with mono-dispersed skin-core beads and layered composite structure in the first year.

For this purpose, we strategically selected hexagonal boron nitride (h-BN) particles and silver coatings on them; the h-BN and silver coated h-BN particles (Ag@h-BN) are used as fillers for insulating layer and EMI shielding layer, respectively (see the schematic in Fig. 16).

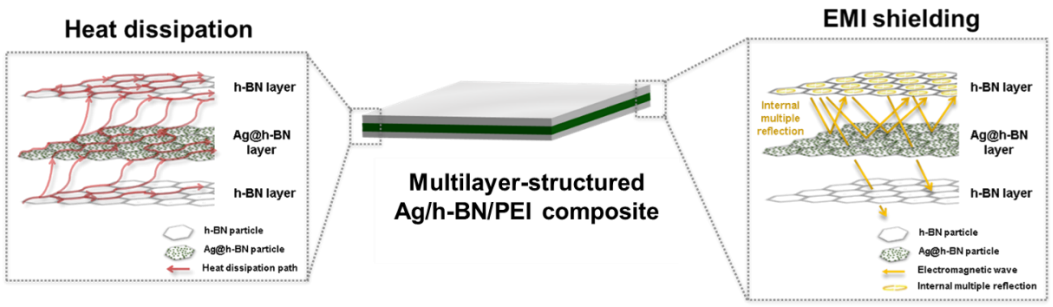

Figure 16. Schematic representation of the multilayer-structured composites for multifunctional properties: Frequency-selective EMI shielding, heat dissipation, and electrical insulation.

The procedure that used to prepare the Ag@h-BN is schematically illustrated in Fig. 17A. First, the h-BN particles were dispersed in silver nitrate solution, which resulted in the adsorption of Ag^+ ions on the negatively charged h-BN particle surfaces through electrostatic attraction. Then, the silver nanoparticles were generated on the surface of the h-BN particles using glucose as a reducing agent. As schematically shown in Figure 17B, the prepared h-BN and Ag@h-BN particles were mixed into NMP/PEI solution (15 wt%) in different volume fractions to yield homogeneous h-BN and Ag@h-BN inks with various viscosities, respectively. After printing process, the samples were dried to remove the residual solvent and yield composites (BN00 and Ag80). The fabricated composites were detached from the substrates with ease. Finally, the BN00 and Ag80 composites were alternately stacked and subsequently compressed under high temperature, yielding 3-layered and 5-layered Ag/h-BN/PEI composites (xL-BN00/Ag80).

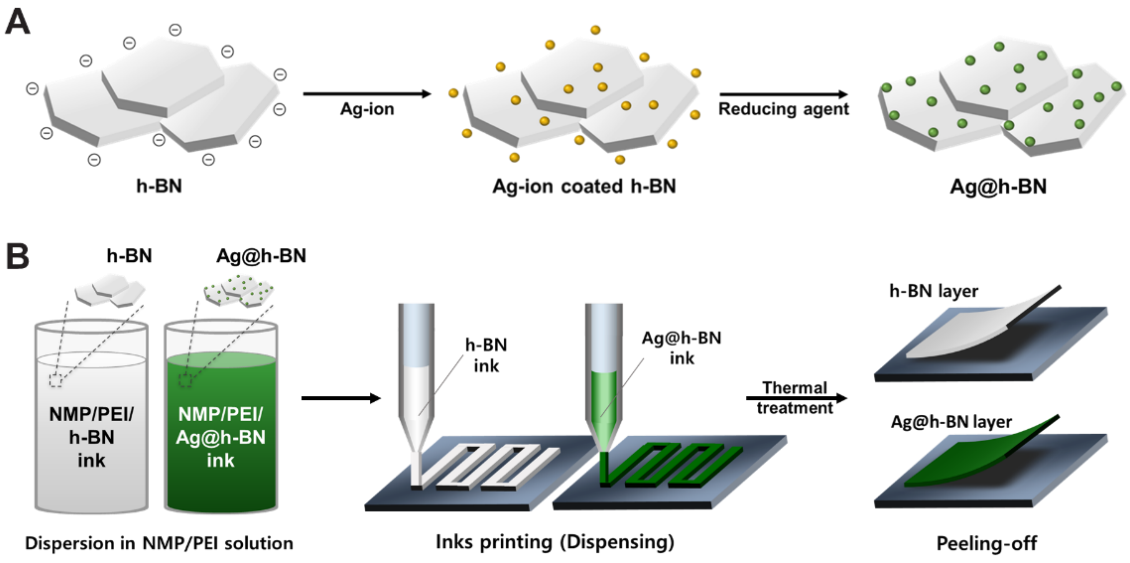

Figure 17. Schematic representation of the procedure used to prepare (A) Ag@h-BN particles and (B) single-layered composite of BN00 and Ag80.

Figure 18 shows SEM images of the h-BN and Ag@h-BN particles at different magnifications. The h-BN particles with an average size of 18 μm have flat and layered structures with a smooth surface (Figure 18A). On the other hand, the surface of Ag@h-BN particles with a plating time of 50 min is very rough, compared to that of h-BN, clearly indicating the formation of silver nanoparticles surrounding the h-BN particles (Figure 18B). With increasing plating time, the silver nanoparticles with sizes ranging from 50 to 200 nm were gradually generated on the surface of h-BN particles. In turn, these nanoparticles met and fused together with neighboring nanoparticles, resulting in formation of continuous silver layers. We used 50 min-plated Ag@h-BN particles to fabricate the Ag80 composite film in this study, since they have continuous silver coating layers and thus could provide electrically conductive paths when applied to composite structures, enabling efficient EMI shielding. As shown in the inset of Fig. 18A and 18B, the color of h-BN powders turns from white to brown after the reduction of Ag^{+} ions due to the formation of silver coating layers.

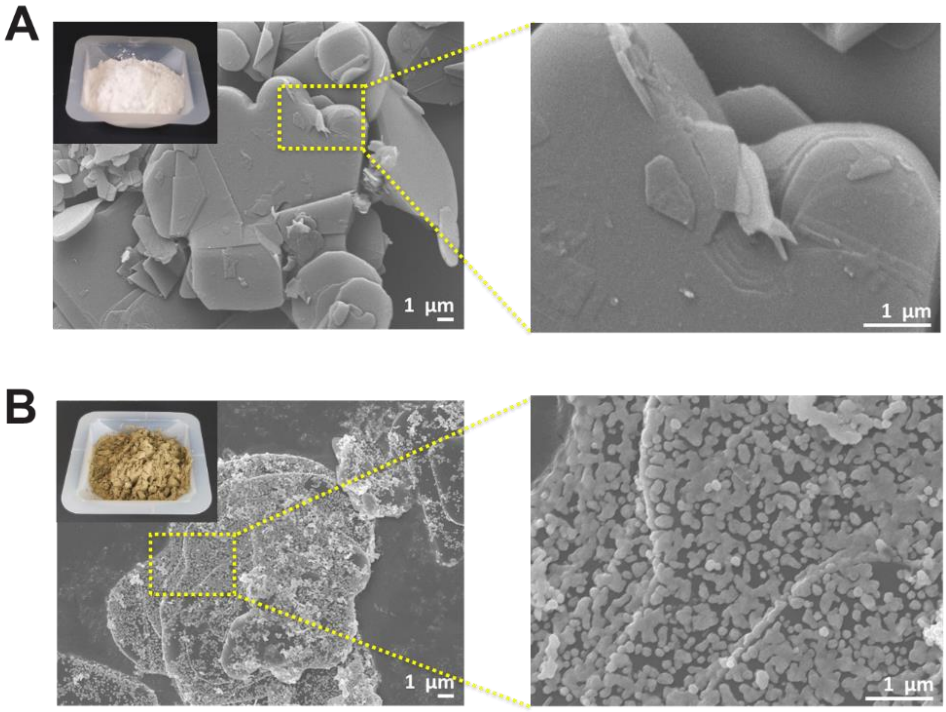

Figure 18. SEM images of h-BN and Ag@h-BN particles at different magnifications; the inset digital images show the corresponding powders.

Fig. 19A shows the cross-sectional digital images of various composites of BN00, 3L-BN00/Ag80, and 5L-BN00/Ag00. The multilayer-structured composites are fabricated by alternatively stacking in the order of BN00 and Ag80 layers followed by compression under high temperature. The optical microscope image of polished interfacial section between the BN00 and Ag80 layers is shown in Fig. 19B. In the BN00 layer, the plate-shaped h-BN particles with around 20 μm are observed. On the other hand, Ag@h-BN particles can be also seen in the Ag80 layer, in which the silver coating layers reflect light showing white color. There are no void or visible cracks, which means that the interfacial bonding between the different composite layers was well-formed under appropriate pressure and heat.

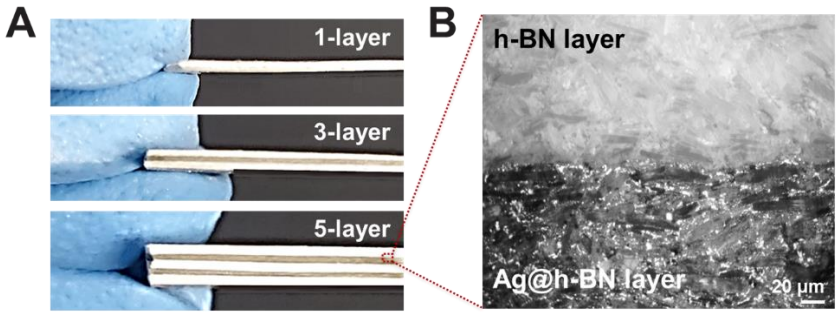

Figure 19. (A) Cross-sectional digital images of various composites of BN00, 3L-BN00/Ag80, and 5L-BN00/Ag00. (B) Optical microscope image of an interfacial section between BN00 and Ag80 layers in layered composite structure.

The total EMI SE of BN00 and Ag80 composites with a thickness of 0.5 mm were first measured in the X-band frequency range to evaluate the ability of h-BN and Ag@h-BN particles to block EM waves, respectively. The SE_T of BN00 composites is relatively low (< 4 dB), transmitting around 50% of the incident EM waves, as shown in Fig. 20A. The SE_T increases linearly with h-BN content. Meanwhile, the Ag80 composite shows significantly improved SE_T of over 24 dB across the measured frequency range, which satisfies commercial EMI shielding requirements (> ca. 20 dB). The improved EMI shielding performance is attributable to the 3-dimensionally connected silver coating layers, which act as an electrical pathway, efficiently shielding EM waves.

Subsequently, we thoroughly investigated the EMI shielding performances of multilayer-structured composites of 3L-BN00/Ag80 and 5L-BN00/Ag00 (Fig 20B and 20C, respectively). Surprisingly, we found that the unique combination of the BN00 and Ag80 layers can realize the frequency-selective EMI shielding capability in the X-band region. Some peaks can be observed, which means that the composite selectively more shield the EM waves in specific frequency. Specifically, increasing h-BN content in the BN00 layer leads to the peak shift to lower frequency region and higher EMI SE in both 3L-BN00/Ag80 and 5L-BN00/Ag80 composites. It is very interesting that the frequency-selective functionality can be controlled with the simply adjusting the h-BN content in the BN00 layer, considering that we identified the h-BN particles are not effective for EMI shielding, transmitting most incident EM waves.

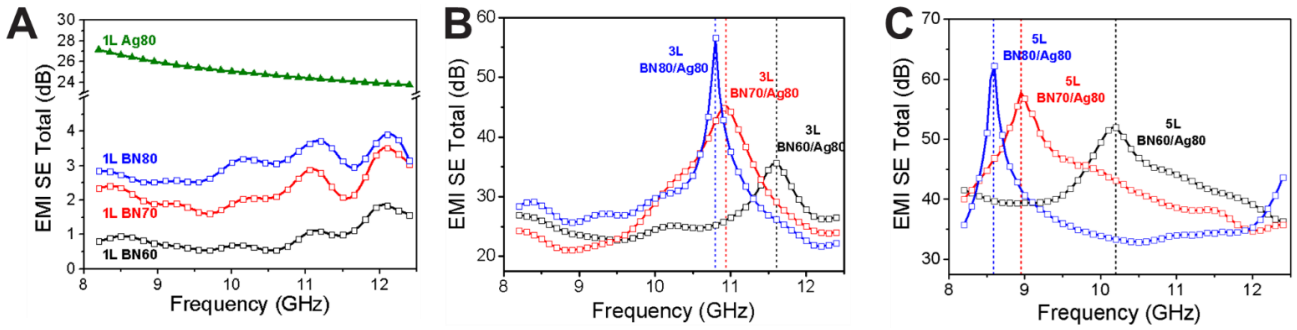

Figure 20. Total EMI SE of (A) single-layered BN00 and Ag80 composites, (B) 3-layered composites (3L-BN00/Ag80), and (C) 5-layered composites (5L-BN00/Ag80) in the X-band frequency range.

The heat dissipation characteristics of the various composites were further confirmed and compared, as shown in Fig. 21. The graphs show the thermal conductivities of BN00, 3L-BN00/Ag80, and 5L-BN00/Ag80 composites in through-plane direction. Typically, since the h-BN is thermally conductive material, the thermal conductivity increases with h-BN content. In addition, the multilayer-structured composite provides higher thermal conductivity than the single-layered composite of BN00, which can be attributable to the presence of Ag80 layers. The Ag80 composite layers would also give excellent heat dissipation property as well as EMI shielding functionality. They may increase the thermal conductivity in the through-plane direction by connecting the thermal paths in the composite structure.

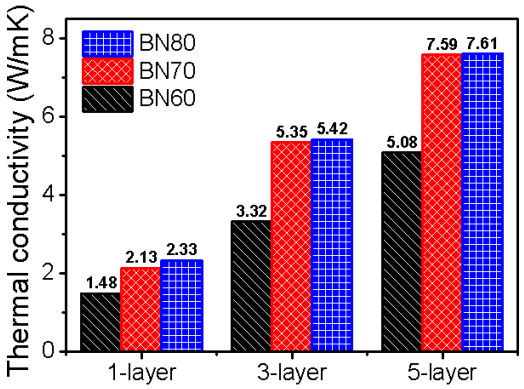

Figure 21. Thermal conductivity of BN00, 3L-BN00/Ag80, and 5L-BN00/Ag80 composites.

Conclusively, we successfully verified that the layered structure can be provide both frequency-selective EMI shielding capability and thermal dissipation property. We believe that this fundamental research in the multilayer-structured composite can used in various applications that require multi-functionality including EMI shielding, heat dissipation, and electrical insulation, etc., opening a new era of advanced EMI shielding materials.

V. PARTICIPANTS

Name	Affiliation Department	Position Field of Study/Final Degree
Jae-Do Nam (PI)	Sungkyunkwan University	Professor
	School of Chemical Engineering Department of Polymer Science and Engineering	Chemical Engineering/Ph.D.
Jonghwan Suhr (Co-PI)	Sungkyunkwan University	Associate Professor
	School of Mechanical Engineering,	Mechanical Engineering/Ph.D.
Uiseok Hwang	Sungkyunkwan University	Ph.D. Student
	Department of Polymer Science and Engineering	Chemical Engineering/B.S.
Na Yeon Kim	Sungkyunkwan University	Ph.D. Student
	Department of Energy Science	Chemical Engineering/B.S.
Donghak Kim	Sungkyunkwan University	M.S. Student
	Department of Polymer Science and Engineering	Chemical Engineering/B.S.
Junyoung Kim	Sungkyunkwan University	Ph.D. Student
	Department of Energy Science	Chemical Engineering/B.S.
Mina Seol	Sungkyunkwan University	M.S. Student
	Department of Polymer Science and Engineering	Chemical Engineering/B.S.

VI. PRODUCTS (PUBLICATIONS)

A. Refereed Journal Articles

Three articles are under preparation and will be published:
– Frequency-Selective Beads: A Novel Composite System for Electromagnetic Interference Shielding
– A Novel Colloidal Ceria Abrasive in the Form of Nanocluster for Chemical Mechanical Planarization (CMP): Surface Morphology, Crystallinity, Surface Activity, and Oxide Removal Rates
– Multilayer-structured Ag/h-BN/PEI Composites for Frequency-Selective Electromagnetic Interference Shielding and Heat Dissipation

B. Patents

Three patents have been filed:
– Composite for frequency electromagnetic interference shielding and electronic device including the same, South Korea-Application/PCT, USA-Under preparation
– Spherical inorganic particles having surface bump and method for preparing same, South Korea-Registration/PCT, Taiwan-Application
– Composite material capable of heat dissipation and shielding electromagnetic wave, electronic device package having the composite material, and method of manufacturing the composite material, South Korea-Application